The use of ellipsometry for studying the adsorption of organic corrosion inhibitors from aqueous solutions on metals. Review. Part 2. Adsorption of salts of organic acids and azoles[1]

N.P. Andreeva,[1] Yu.I. Kuznetsov[1]* and Kh.S. Shikhaliev[2]

[1]A.N. Frumkin Institute of Physical Chemistry and Electrochemistry, Russian Academy of Sciences, Leninsky pr. 31, 119071 Moscow, Russian Federation
[2]Voronezh State University, Universitetskaya pl. 1, 394018 Voronezh, Russian Federation
**E-mail: yukuzn@gmail.com*

Abstract

In the first part of this review, a technique for obtaining adsorption isotherms by the ellipsometric method was presented and a brief analysis of theoretical adsorption isotherms was given. Analyzing the literature in which the ellipsometric method was used, we noted that it was used mainly to determine the thicknesses of adsorbed layers. In the second part of the review, we will consider examples of studying the adsorption of well-known organic corrosion inhibitors (CIs) on the metal surface using this method. These include salts of carboxylic and phosphonic acids, organophosphates (salts of acid dialkyl phosphates), and azoles. An important advantage of using ellipsometry in aqueous or aqueous-organic solutions is the possibility of its combination with electrochemical measurements. It makes it possible to study adsorption in a wide range of potentials. Examples of adsorption of a mixture of CIs and induced adsorption are given, the possibility of enhancing the adsorption of BTA by small additions of dimegin to a solution on iron and copper is shown. Depocolin has been proposed as a surface modifier for copper and MNZh5-1 alloy. The conditions for preparing the surface of magnesium and aluminum to obtain adsorption isotherms are considered in detail. Adsorption isotherms of the following sodium salts of higher carboxylic acids were obtained on magnesium: sodium oleyl sarcosinate, sodium oleate, and sodium linoleate from a borate solution with pH 11.2. Determination of the thicknesses of the adsorbed layers suggests their location on the surface. The thicknesses of the adsorbed layers of depocolin and dimegin on nickel determined by the ellipsometric method and XPS coincide within the measurement error. For some inhibitors, kinetic adsorption isotherms have been obtained, which can be adequately described by the Roginsky–Zeldovich slow chemisorption equation.

Received: March 28, 2023. Published: May 11, 2023 doi: 10.17675/2305-6894-2023-12-2-10

Keywords: *ellipsometry, adsorption isotherms, Temkin isotherm, XPS, dimegin, depocolin, BTA, sodium N-phenylanthranilate, oleyl sarcosinate, sodium oleate, kinetic adsorption isotherms.*

[1]The study received financial support from the Ministry of Science and Higher Education of the Russian Federation within the framework of State Contract with universities regarding scientific research in 2022–2024, project No. FZGU-2022-0003.

Salts of carboxylic acids

This article is a continuation of our review, in the first part of which [1] the procedure for obtaining the adsorption isotherms of organic compounds by the ellipsometric method is considered and a brief analysis of the theoretical adsorption isotherms is given. The influence of the chemical structure of carboxylate CIs: sodium benzoate and phenylanthranilate (SPhA) on the effectiveness of their protection against corrosion of zone-melted iron, Fe-ARMCO, low-carbon steel St3 in aqueous solutions is considered in [2] and reviews [3, 4]. In [5], the adsorption from aqueous solutions of substituted of SPhA, $C_6H_5NHC_6H_4COONa$ was studied. They are sodium salt of aromatic amino acids: mephenamic acid *o*-[2,3-$(CH_3)_2C_6H_3NH]C_6H_4COOH$ (SMEPh); *N*-(3-difluoromethyltiophenyl)-anthranilic acid *o*-[3-$(SCHF_2)C_6H_4NH]C_6H_4COOH$, iso-diphtorant, (DPh); and fluphenamic acid *o*-[3-$(CF_3)C_6H_4NH]C_6H_4COOH$ (SFPh). Changes in the angle $\delta\Delta=(\Delta-\Delta_0)$, where Δ and Δ_0 are the current and initial values of the angle, respectively, and the adsorption isotherms constructed from them are represented in Figure 1. The error in determining the standard free energy of adsorption $\left(-\Delta G_a^0\right)$ usually does not exceed 5%. The values of $\left(-\Delta G_a^0\right)$ and hydrophobicity[2] (log*P*) of these compounds are given in Table 1.

The CI's hydrophobicity plays a major role in its effectiveness. The higher the *P* value, the more hydrophobic the compound is. The log*D* coefficient is the ratio of the sum of the concentrations of all forms of the compound (ionized and non-ionized) in each of the two phases and depends on the pH of the aqueous phase:

for acids $$\log D = \log P - \log\left[1+10^{(\mathrm{pH-p}Ka)}\right] \quad (1)$$

for bases $$\log D = \log P - \log\left[1+10^{(\mathrm{p}Ka-\mathrm{pH})}\right] \quad (2)$$

With an increase in the hydrophobicity of the three compounds studied, the value of $\left(-\Delta G_a^0\right)$ increases. For example, SDPh (σ=0.33 for the $SCHF_2$ group) is adsorbed much better than SPhA (σ_H=0.00), but noticeably more weakly than SFPh (σ_{CF3}=0.43).

It can be seen that adsorption becomes stronger with the increase in their polarity reflected by Hammett's σ-constants [7, 8]. SMEPh contains two electron-donating CH_3 groups as substituent *R*, while SFPh has a strong electron-withdrawing CF_3 group. However, in both cases, the protective properties of CI increase significantly.

In [9], the adsorption and protective properties of SFPh on the St3 surface in a neutral borate buffer solution were studied using electrochemistry, ellipsometry, and XPS methods. The adsorption layer thickness *d* was determined on the oxidized surface at *E*=0.2 V (*d*=0.8 nm) and on the reduced surface *E*=–0.65 V (*d*=0.5 nm). Analysis of ellipsometric

[2] The criterion of hydrophobicity is the logarithm of the distribution coefficient of the test compound in the system of two immiscible liquids octanol-water, log*P* [6, 7]. Here $P=N_0/N_{aq}$, where *N* is the molar fraction of the chemical compound in octanol and water, respectively.

and XPS data has shown that SFPh forms a monomolecular layer both on bare and oxidized surface of mild steel, which thickness corresponds to the size of SFPh molecule. The angle resolved XPS allowed determining the vertical orientation of SFPh molecules that are anchored to iron cation by oxygen of carboxyl group and CF_3 groups form the topmost layer. It seems that the layer formed by SFPh or similar molecules may serve as a robust interface for grafting other substances onto such a functionalized surface.

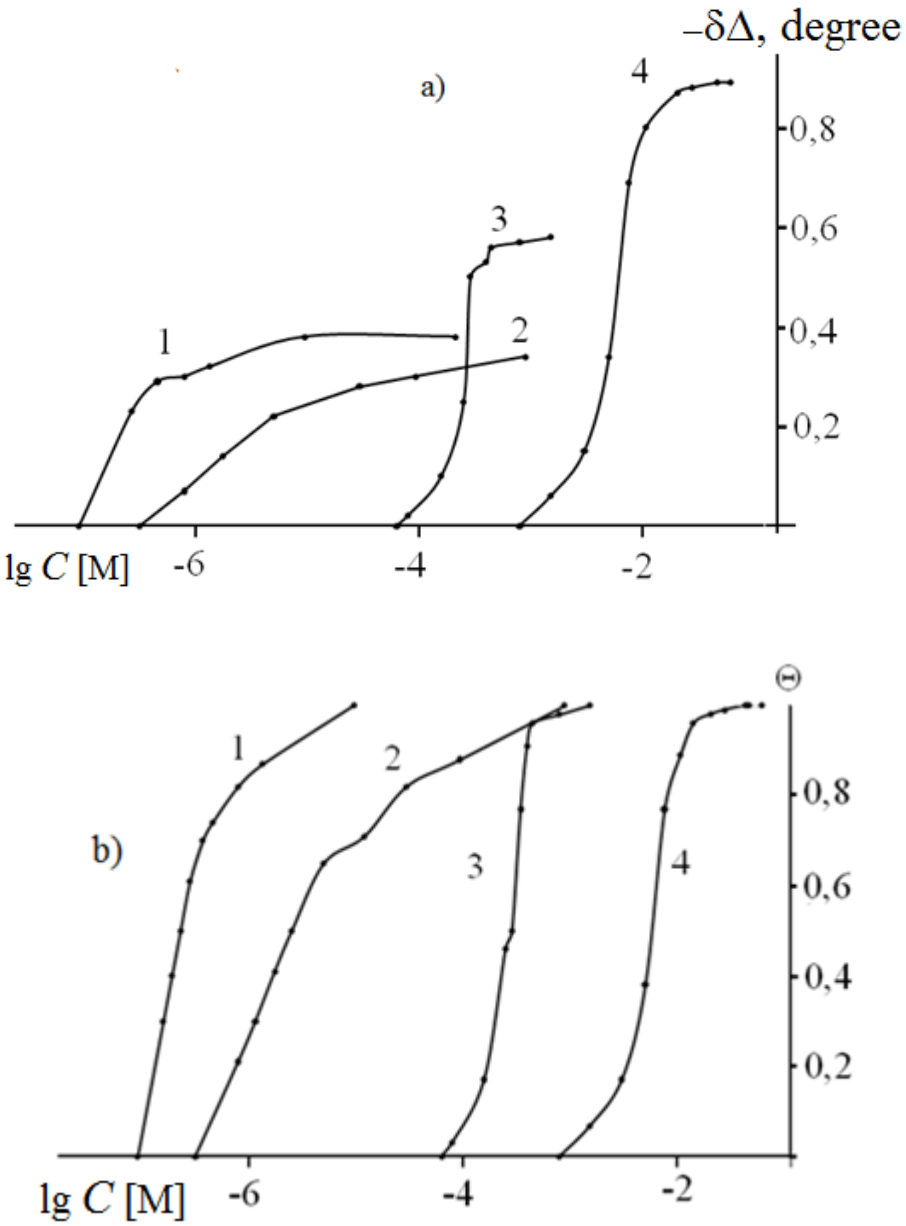

Figure 1. Dependence of the change in the ellipsometric angle (Δ) (a) and surface coverage (b) *vs*. lg*C* of SFLPh (1), SDPhT (2), SMEPh (3) and SPhA (4) on oxidized iron surface at E=0.2 V in borate buffer with pH 7.4.

Table 1. The standard free energy of adsorption values for the anions of sodium salts of substituted SPhA derivatives on zone-melted iron from a borate buffer pH 7.4 at $E=-0.65$ and 0.20 V, as well as the logarithm of the distribution coefficients (log$P$), and (log$D$) calculated using the ACD/Labs 6.00 program (build 6.12/17 Sep 2002).

Inhibitor	$\left(-\Delta G_a^0\right)$ **kJ/mol at:**	
	$E=-0.65$ **V**	$E=0.2$ **V**
SPhA: log$P=4.41\pm0.41$ log$D=1.32$	15.6	16.8
SMEPh: log$P=5.33\pm0.42$ log$D=2.29$	40.5	27.3
SDPh: log$P=4.99\pm0.59$ log$D=1.94$	45.7	46.0
SFPh: log$P=5.62\pm0.48$ log$D=2.57$	56.5	49.6

The use of mixed CIs often allows for lower concentrations to be used, reducing the risk of environmental pollution and the cost of CI protection of metals. This justifies the increased interest in composite CIs, including those of the adsorption type [2, 10]. Anions of substituted sodium phenylantranilates ($NaCOOC_6H_4NHC_6H_4R$) when used together with higher organic carboxylates such as $CH_3(CH_2)_7CH=CH(CH_2)_7COONa$ (sodium oleate, SOl), for mixtures of aromatic amino acids with sodium phenylundecanoate $C_6H_5(CH_2)_{10}COONa$ (SPhU), $C_{10}H_6(COONa)$ sodium hydroxynaphthoate (SHN), cause an increase in metal protection only if they themselves are sufficiently hydrophobic (SPhA, SMEPh). Figure 2 shows that SHN and SMEPh have similar adsorption properties (on oxidized iron, their values are $\left(-\Delta G_a^0\right)=27.6$ and 27.2 kJ/mol, respectively). The molecular masses of the components are almost equal, therefore, in the first approximation, the average value (219.8) can be taken as the mass of their equimolar mixture and a conditional isotherm can be constructed. In this case, an increase in adsorption upon passing from individual CIs to their equimolar mixture in the region of medium occupancies becomes obvious. The equimolar composition is also interesting, in which, instead of SHN, a more surface-active SPhU with $\left(-\Delta G_a^0\right)=33.1$ kJ/mol is used. In this case, the mixed CI isotherm sharply shifts to the left. For a mixture of SMEPh and SPhU, the CI adsorption strength reaches a much higher value $\left(-\Delta G_a^0\right)=41.7$ kJ/mol.

Further ellipsometric studies of CIs adsorption showed that mutual enhancement is due to the ability of one component to initiate the adsorption of the other. Thus, if SPhU is first adsorbed on the electrode, for example, up to the degree of coverage $\Theta=0.2$ or 0.5, and only then SMEPh is introduced into the solution, then the adsorption increases, yet the stronger, the higher the preliminary adsorption of SPhU is [11]. To achieve this, after the formation

of a monolayer of SPhU on oxidized iron at E=0.2 V, without turning off the potentiostat, the solution was replaced with pure borate buffer. Since SPhU is chemisorbed on this electrode, its desorption proceeds slowly, and even with the subsequent introduction of SMEPh into the solution, no signs of displacement of SPhU from the surface of oxidized iron were observed.

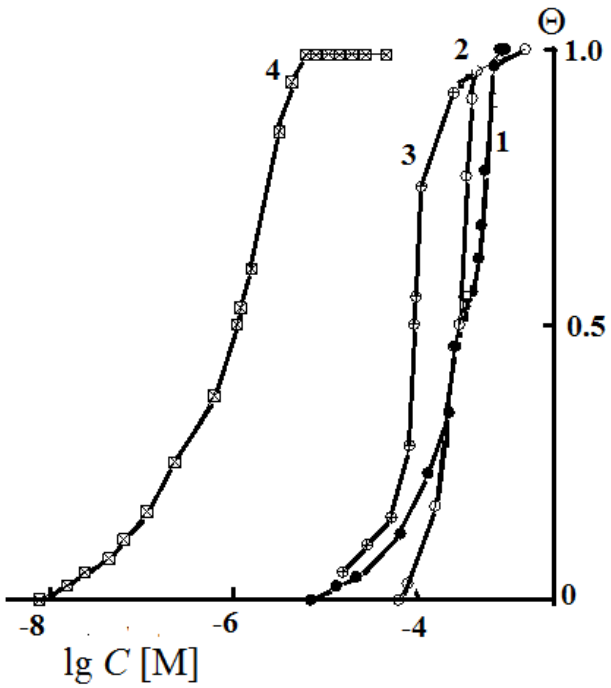

Figure 2. Isotherms of adsorption of sodium salts of organic acids and their mixtures: (1) SHN, (2) SMEPh, (3) SHN+SMEPh (1:1), and (4) SPhU+SMEPh (1:1) on oxidized iron surface at E=0.2 V in borate buffer with pH 7.4.

By taking the surface of the electrode coated with a SPhU monolayer as the initial one and increasing the concentration of SMEPh, we obtained the adsorption isotherm of the latter (Figure 3). It is also possible to adsorb a third layer consisting of SPhU anions onto such an electrode. To do this, after completion of the coating of oxidized iron with a SMEPh monolayer, maintaining E=0.2 V on the electrode, the solution was changed back to pure buffer, and then SPhU was introduced into it.

In [12], the passivation of iron and low-carbon steel in a borate buffer solution with pH 7.4 of 1,2,3-benzotriazole $C_6H_5N_3$ (BTA) and its equimolar composition with SPhU was studied. BTA practically does not prevent local depassivation of steel by chloride anions. The equimolecular mixture SPhU+BTA surpasses its individual components in adsorption capacity on oxidized iron. The adsorption of all three CIs was formally described by the Frumkin equation. In [13], a theoretical description of the joint adsorption of surface-active components of a solution on a metal electrode is given when the concentration of one of the components in the solution is constant. In [12], we performed a comparative analysis of attraction interactions between adsorbed SPhU and BTA particles using this method. The

results of the analysis enabled us to suggest that adsorption of mixture on passive iron (E=0.2 V) causes attraction not between the same adsorbate particles but between SPhU and BTA anions.

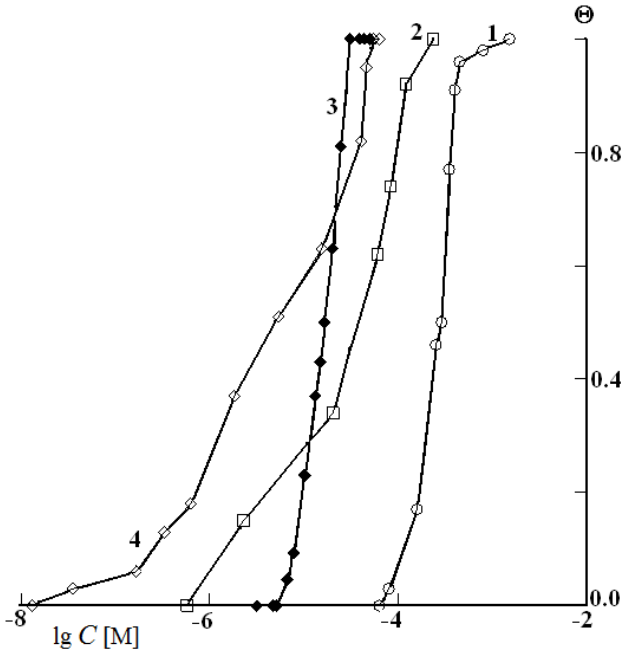

Figure 3. Isotherms of adsorption of sodium salts of organic acids and their mixtures on oxidized iron surface at E=0.2 V in borate buffer with pH 7.4: (1) SMEPh without and (2) with preliminary adsorption of SPhU, and (3) SPhU without and (4) with preliminary formation of a two-layered coating consisting of SPhU+SMEPh.

Some difficulties arose in the study of the adsorption of sodium salts of higher carboxylic acids on magnesium: $CH_3(CH_2)_7CH{=}CH(CH_2)_7CON(CH_3)CH_2COONa$ – sodium oleyl sarcosinate (SOS); $CH_3(CH_2)_7CH{=}CH(CH_2)_7COONa$ – sodium oleate (SOl); $CH_3(CH_2CH{=}CH)_3(CH_2)_7COONa$ – sodium linoleate (SLi) [14]. This metal is very active, its standard electrode potential, $E^0_{Mg/Mg^{2+}} = -2.37$ V, is indicative of a high thermodynamic possibility of oxidation and corrosion of the metal. The difficulty of realizing the condition of a stable state of the magnesium surface, which is necessary for measuring adsorption on it by the ellipsometric method, required a special preliminary passivation of the electrode. In order to ensure a stable surface (the constancy of ellipsometric angles Δ and Ψ), magnesium electrode was subjected to special preliminary passivation. First, the electrode was stripped, polished, and degreased before being chemically oxidized in 5.0 M NaOH solution for 1.5 h. Next, it was transferred to the working solution (a borate buffer with pH 11.2), where it was left for additional 17 h. The electrode's surface retained a high gloss after this treatment. After 17 h, a potentiostat was used to maintain the electrode potential at 20 mV more negative than the corrosion potential E_{corr}. After angles Δ and Ψ became stable, the concentrated CI solution was added to the cell. For each concentration of CI (C_{inh}), angle

Δ was measured over time until it became constant. For every change in C_{inh}, the angle was $\delta\Delta=\Delta-\Delta_0$ where Δ is the current angle obtained after the CI additive was introduced into the solution, with Δ_0 is the initial value.

The thickness of the oxide layer was determined numerically, as shown in part 1, [1] for the growth of oxides on copper. For this, a theoretical nomogram of the growth of MgO oxide on the plane Δ–Ψ (Figure 4) with $N_{film}=1.45$ was constructed. The refractive index of magnesium was determined in a solution and in air. For λ=640 nm and φ=68.5°, $N_{Mg}=0.85-3.46i$ was calculated. The theoretically constructed oxide growth nomogram shows the experimentally obtained values of the angles Δ and Ψ. The points on the curve are drawn every 5 nm; the arrow indicates the moment of CI introduction. The thickness of the oxide film on the surface of magnesium reaches about 70 nm in a 5 M solution of NaOH and about 50 nm in a borate solution with pH of 11.2, over 120 min.

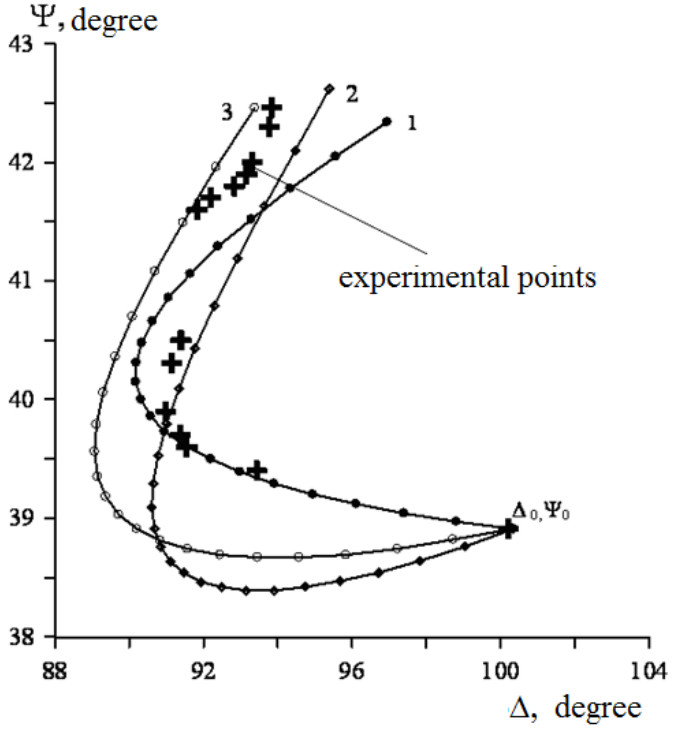

Figure 4. The nomographic chart on the Δ–Ψ plane. The theoretical curves are constructed for the growth of an oxide with N_{film}=(1) 1.45–0.02*i*, (2) 1.42–0.05*i*, and (3) 1.45–0.05*i*. The points in the curves are drawn every 5 nm. (+) denotes the experimental values of the angles.

The adsorption of the anions of these salts was adequately described by the Temkin equation, which yielded the following adsorption energies: SOl $\left(-\Delta G_a^0\right)$=57.2 kJ/mol, SLi $\left(-\Delta G_a^0\right)$=60.1 kJ/mol, SOS $\left(-\Delta G_a^0\right)$=63 kJ/mol. It can be observed that chemisorption of the investigated CIs takes place here, with the strength increasing in the series: SOl < SLi < SOS. Interestingly, the order of increasing hydrophobicity of the adsorbate

molecules characterized by the log*P* value is different: SLi (6.50) < SOS (6.57) < SOl (7.70). A similar series is maintained for $\left(-\Delta G_a^0\right)$ and log*D*: SOS (3.17) < SLi (3.91) < SOl (5.1).

The adsorption of SOS was studied on zinc from a neutral borate buffer with pH 7.4 [15]. On the oxide-free zinc surface at $E=-0.9$ V, the adsorption isotherm was adequately described by the Temkin logarithmic isotherm. The values $\left(-\Delta G_a^0\right)=45.3$ kJ/mol and $f=1.2$ were obtained, and on the pre-oxidized electrode at $E=0.2$ V $\left(-\Delta G_a^0\right)=49.3$ kJ/mol and $f=2.6$. The value of $\left(-\Delta G_a^0\right)$ on zinc is higher than on iron (35.9 kJ/mol) but lower than on copper (62 kJ/mol).

The thickness of the SOS monolayer is estimated to be approximately 3.0 nm on the surface of oxidized zinc and 0.5 nm on the "clean" surface. For comparison, the size of the SOS molecule determined by summing the bond lengths is 2.9 nm. This allows us to conclude that the adsorbed SOS anions on oxidized zinc are oriented vertically to the electrode surface, but in the absence of an oxide film, their orientation becomes inclined.

The adsorption of another known CI, SFLPh, on the oxidized zinc surface at $E=0.2$ V was also studied in neutral (pH 7.4) and weakly alkaline (pH 9.1) borate solutions also by the ellipsometric method [16]. The study of the kinetics of zinc oxidation for 120 min showed that in the first case, the thickness of the oxide reaches ~4 nm, and in the second case, ~1.2 nm. The oxide layers formed in a weakly alkaline environment are more compact than those formed in a neutral buffer. However, the thicknesses of SFLPh adsorption films turned out to be the same in both cases, ~1.3 nm. The adsorption of SFLPh on the zinc surface was described by the Frumkin isotherm. SFLPh adsorption is more efficient in a slightly alkaline medium, as indicated by a higher value $\left(-\Delta G_a^0\right)=61$ kJ/mol than in a neutral solution $\left(-\Delta G_a^0\right)=57.8$ kJ/mol. At the same time, the chemisorption of SFLPh anions in both media is beyond doubt, and its strength is confirmed by the results of XPS studies of the zinc surface after its passivation with a solution of this CI.

Sodium salts of many carboxylic acids can be used to protect copper and its alloys from corrosion. For example, in [17], studies were carried out comparing the adsorption properties of several sodium salts of higher carboxylic acids (non-oxidizing type) on copper. The effectiveness of protecting copper from corrosion under harsh conditions of 100% relative atmospheric humidity with daily moisture condensation on samples was also investigated by passivating adsorption films. Figure 5 shows changes in the value of $(-\delta\Delta)$ as a function of the logarithm of the concentration of five carboxylates on oxidized copper in a borate buffer with pH 7.4 at $E=0.2$ V.

As shown by ellipsometric measurements, SOS anions begin to be adsorbed on oxidized copper in the region of very low $C_{inh}\geq 0.02$ nmol/L, and after the formation of a monolayer, a multilayer film is also formed. This is not surprising, since SOS is a well-known colloidal surfactant, which is not only low toxic, but also easily biodegradable, and therefore is widely used in the industry [18]. Adsorption upon filling the first monolayer with CI is adequately described by the Frumkin isotherm equation with $\left(-\Delta G_a^0\right)=62$ kJ/mol.

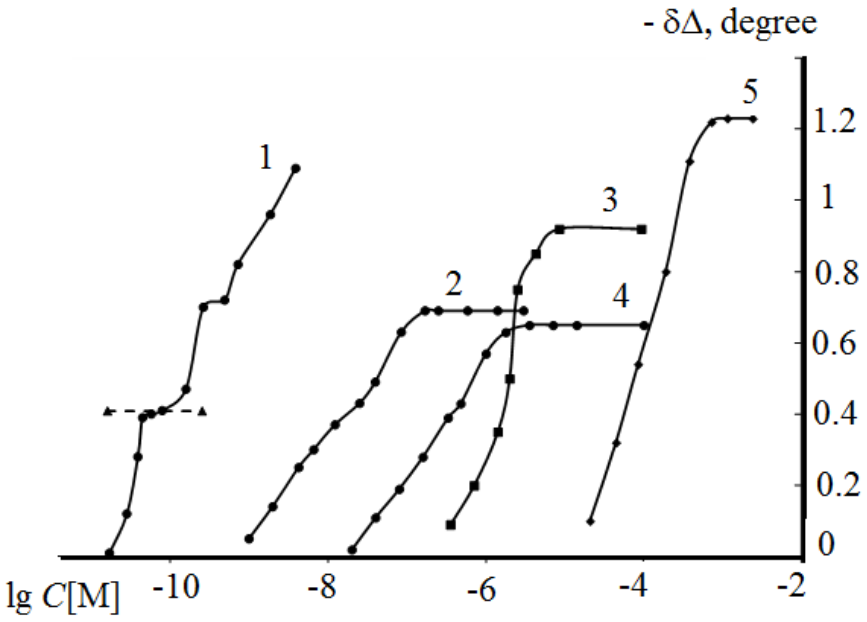

Figure 5. Dependence of the change in the ellipsometric angle on lg*C* of (1) SOS, (2) SOl, (3) SMEPh, (4) SFLPh, and (5) SPhU on a copper surface at E=0.0 V in borate buffer, pH 7.4.

Another CI with a high adsorption capacity is SOl, although it begins to be adsorbed at log$C$=−9.0, which is 1.5 orders of magnitude higher than for SOS. The formation of two SOl layers occurs in the range logC_{SOl}=−(6.77–5.52). In the region of higher C_{SOl}, the formation of multilayers is possible, similarly to how it happened on iron [11].

The adsorption of SOl during the formation of the first monolayer is also well described by the Frumkin equation, but with a smaller value of $\left(-\Delta G_a^0\right)$=57 kJ/mol. Both CIs appear to be chemisorbed on the oxidized electrode surface. The same conclusion can be drawn by estimating the $\left(-\Delta G_a^0\right)$ value for SFLPh and SMEPh (48 and 43 kJ/mol, respectively).

Corrosion testing of copper plates treated with dilute (2.0 nmol/L) solutions of the studied carboxylates at room temperature showed that SOS under the above severe conditions prevents the appearance of the first signs of corrosion significantly better than other CIs. Judging by the time before the appearance of the first corrosion site in a humid atmosphere, the efficiency of SOS (21 days) is 3–3.5 times higher than that of SFLPh or SPhU. The protection of copper not only by SOS, but also by SOl (τ=17 days), is apparently accompanied by self-organization in adsorption layers, since its efficiency increases significantly with an increase in the duration of the passivation treatment of copper. When the passivation time is reduced to 5 min, the first centers of corrosion on copper samples during subsequent tests are formed much earlier, since the CI film does not have time to form in such a time. By increasing the temperature to 60°C and 5 min of passivation treatment is enough to provide τ=23 h. Studies on non-toxic CIs for replacement of classical molecules containing sulfur, nitrogen or aromatic functions such as BTA to protect copper from corrosion are of considerable interest. In [19], a study on the conditions and mechanism of copper corrosion inhibition by linear sodium heptanoate with the formula

$CH_3(CH_2)_5COONa$ is reported. Sodium heptanoate has been proven to be a good non-toxic CI for copper corrosion and its optimum operating conditions, pH 8 and 0.08 mol/L NaC_7, are compatible with the water of a heat exchanger. The inhibition is due to the formation of a thin metallic soap layer mainly constituted by copper heptanoate. ECAFM techniques have shown the relations between the inhibition efficiency and the morphology of the surface layer under real conditions. Furthers studies dealt with the determination of the relationship between the orientation of the copper substrate and the growth of metallic soaps. The passivation of copper in 0.08 mol/L sodium heptanoate solution with pH 8 was studied by ellipsometry [20]. The inhibition may be due to the formation of a passive layer containing $Cu(OH)_2$ and Cu(II) heptanoate $[CH_3(CH_2)_5COO]_2Cu$ (designated as $Cu(C_7)_2$) on the copper surface. Two growth rates are observed during the passivation process. A model of a duplex layer is proposed. The thickness of the passive film is evaluated as 14±1.5 nm.

Salts of dicarboxylic acids containing two reactive carboxyl groups are also of great interest. They do not pose an environmental hazard, since they are found in nature in a free form (green parts of plants and juice), and if they show protective properties, they can be classified as "green Cis". It turned out that they can be strongly adsorbed on the surface of metals [21]. The adsorption of (sodium malonate $NaOOCCH_2COONa$, ethylmalonate $NaOOCCH(C_2H_5)COONa$, and sodium succinate $NaOOCCH_2CH_2COONa$) on copper was studied in [22]. The values $\left(-\Delta G_a^0\right)$ calculated from the full Temkin isotherm are 47.7, 69.4, and 77.4 kJ/mol, respectively. It can be assumed that the high adsorbability of these anions is due to the participation of both carboxyl groups of these anions in their chemisorption process with the copper surface. For substituted malonates, this interaction should also be facilitated by the close spatial arrangement of carboxyl groups in their molecules.

Noteworthy are studies of the adsorption, electrochemical, and corrosion behavior of copper in aqueous solutions of sodium salts of alkylmalonic acids (AMA) with alkyl lengths n=0, 2, 4, 7, and 9 [23]. This work used ellipsometry, electrochemical impedance spectroscopy (EIS), potentiodynamic polarization measurements and corrosion tests. Addition of alkylmalonic acid salts at a concentration of C_{inh}=0.002 mol/L to borate buffer solution (pH 7.4) containing 0.01 mol/L NaCl slows down the anodic dissolution of copper, increases its local depassivation potential and inhibits the cathodic oxygen reduction. Figure 6 presents polarization curves of copper in borate buffer solution pH 7.4 containing 10.01 mol/L chloride without (1) and with addition of 3 mmol/L AMA. The greater the alkyl length in the CI, the more expressed these effects are. It has been shown that the adsorption strength of alkylmalonate increases with increasing alkyl length and is adequately described by the full Temkin isotherm equation. The value of $\left(-\Delta G_a^0\right)$ of these anions on the oxidized copper surface at E=0.0 V is 47.7 kJ/mol for malonic acid and 83.9 kJ/mol for nonylmalonic acid, which suggests a chemical nature of adsorption.

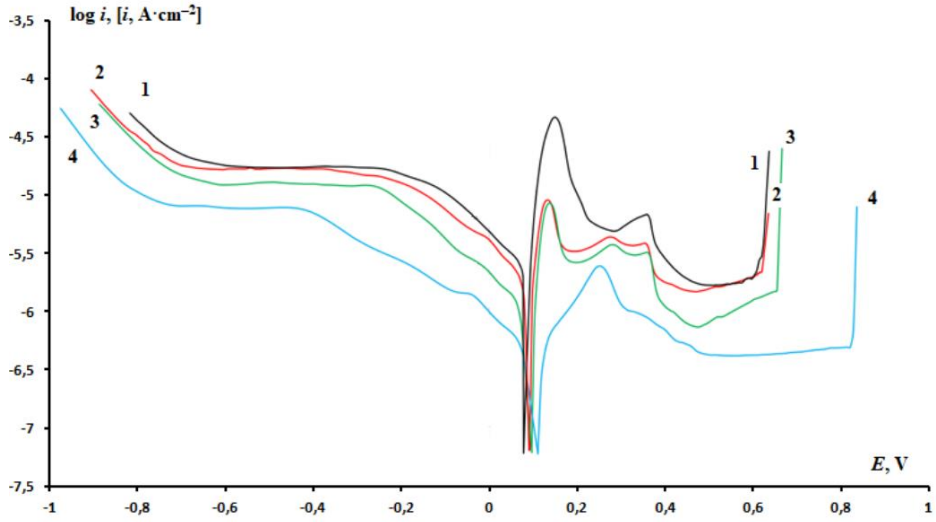

Figure 6. Polarization curves of copper in borate buffer solution with pH 7.4 containing 10 mmol chloride without (1) and with addition of 3 mmol/L OCI: C_0 (2), C_2 (3) and C_9 (4).

An even more complicated case is the adsorption on metals and inhibition of corrosion by salts of dicarboxylic and even polycarboxylic acids of macrocyclic organic compounds. Since organic compounds are capable of transferring their electrons to unoccupied d-orbitals of a metal, forming covalent bonds with it, or, conversely, accepting free electrons from the metal surface, it is not easy to predict which functional groups containing N, O, S, and P heteroatoms are active centers that carry out bonding of large organic molecules or ions to a metal surface.

It should be recognized that the adsorption of such salts of di- or polycarboxylic acids using ellipsometry is much less studied. In this regard, macroheterocyclic compounds, such as porphyrins and phthalocyanines, are of great interest [24–27]. The assessment of adsorption, for example, by phthalocyanines, which in [25] were represented by 1(4)-tetrakis[(2-mercapto)pyridine]phthalocyanine (I) and 2,3-octakis[(2-mercapto)pyridine]-phthalocyanine (II) sulfates, was estimated in 0.1 M/L HCl solution by electrochemical method from the increase in the charge transfer resistance R_s with an increase in the CI concentration. The adsorption of the studied phthalocyanines on the aluminum surface was adequately described by the Langmuir equation with the value $\left(-\Delta G_a^0\right)$=24.2 kJ/mol and decreased with increasing temperature. Both of these facts point to the physical adsorption of phthalocyanines on the aluminum surface, at least from an acidic solution.

Apparently, the adsorption of Dimegin (DMG) on the passive surface of zone-melted iron (with an impurity of C<0.001%) from a borate buffer with pH 7.4 was studied by the ellipsometric method for the first time [28]. DMG macrocyclic compound [disodium salt of 2,4-di(metoxyethyl)deuteroporphyrin IX] (Figure 7a). It was shown that its adsorption on an iron electrode at E=0.2 V resulted in the formation of a monomolecular layer strongly bound to the surface of oxidized iron. It is described by a logarithmic Temkin equation with the

values $\left(-\Delta G_a^0\right)$=43.3 kJ/mol and f=1. The authors compared these adsorption characteristics with those for BTA, a well-known CI for copper. The adsorption of BTA under the same conditions on passive iron is adequately described by the same equation, but with a much smaller $\left(-\Delta G_a^0\right)$=19.2 kJ/mol and a larger value of f=3.6. Unlike BTA, which is rather weakly adsorbed on iron in a neutral aqueous solution, *i.e.*, does not chemically interact with the electrode surface, DMG is chemisorbed on passive iron with high probability. In this regard, DMG chemisorption was used to modify the surface in order to improve the adsorption of BTA on it.

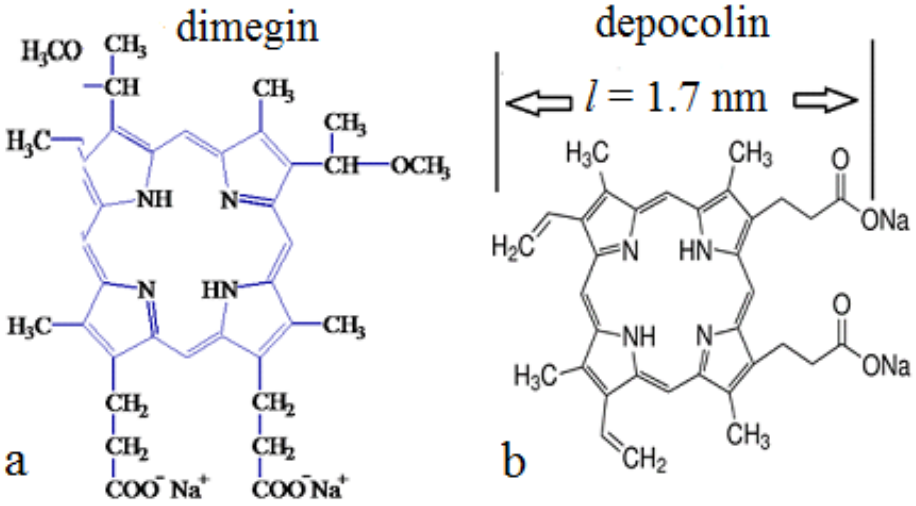

Figure 7. Structural formulas of dimegin and depocolin.

Indeed, such a modification of the iron surface improves the adsorption of BTA on it and increases $\left(-\Delta G_a^0\right)$ from 19.2 to 45.1 kJ/mol. The adsorption characteristics of BTA, as can be seen from the results of their measurement at various degrees of coverage the iron surface with DMG (Θ_{DMG}), are presented in Table 2. When passing to the modified surface, the factor of its inhomogeneity, characterized by the value f, first increases (up to Θ_{DMG}~0.5), and then decreases. Θ_{DMG} has a similar effect on the value $\left(-\Delta G_a^0\right)$, which is also maximum at Θ_{DMG}~0.5, but even at Θ_{DMG}=1.0 it is more than 2 times higher than the similar value for BTA adsorption on the unmodified surface of the passive gland. The corresponding BTA adsorption isotherms are shown in Figure 8.

During the adsorption of BTA on passive iron, small changes were observed $|\delta\Delta|$~0.18° corresponding to its film thickness of 0.4–0.5 nm, which indicates a flat arrangement of BTA molecules on the electrode surface. The ellipsometric measurements also showed an almost flat arrangement of DMG $|\delta\Delta$~0.41°| corresponding to a thickness of ~0.9 nm.

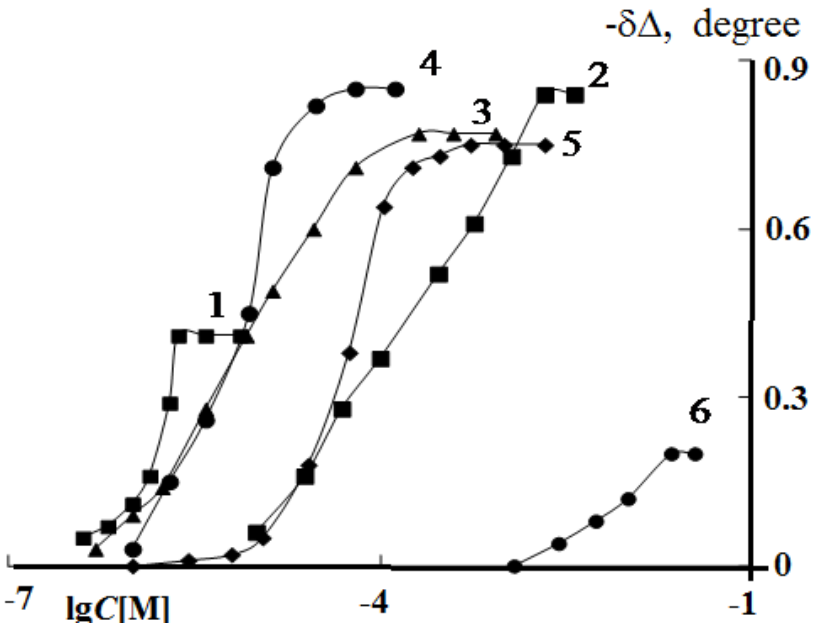

Figure 8. Dependence of the change in the ellipsometric angle on lg*C* of (1) dimegin concentration; (6) BTA on iron surface oxidized at E=0.2 V in borate buffer, pH 7.4; and BTA on an iron electrode preliminarily modified by dimegin adsorption, degrees of electrode surface coverage, Θ_{DMG}: (2) 0.27; (3) 0.50; (4) 0.70; and (5) 1.0.

Table 2. Adsorption characteristics of BTA by varying the degree of coverage with dimegin (Θ_{DMG}) of the surface of oxidized iron.

Θ_{DMG}	f	$\left(-\Delta G_a^0\right)$, kJ/mol
0.00	3.6	19.2
0.27	5.1	38.7
0.50	5.0	45.1
0.70	4.9	44.6
1.00	4.7	39.9

The thickness of the adsorbed BTA layer increases if it is formed on a passive electrode at the same E=0.2 V, the surface of which is preliminarily filled with DMG, even partially. For all studied Θ_{DMG}, the thickness of the adsorbed BTA layer reaches 1.0–1.2 nm. This indicates that the BTA orientation is no longer flat.

As we showed later [29], DMG is adsorbed from a borate buffer with pH 7.4 on passive copper at E=0.0 V even more strongly than on iron. DMG adsorption on oxidized copper occurs at low concentrations, lg C_{inh}=−7.75...−5.75, is also well described by the Temkin equation with the values $\left(-\Delta G_a^0\right)$=56 kJ/mol and f=3.4. Such a strong binding of DMG to the copper electrode raises no doubts about its chemisorption. It is no coincidence that it surpasses many known copper CIs (SFLPh, BTA and even its more effective derivative 5-

Cl-BTA) in terms of passivating and protective action. This makes it possible to use very low concentrations of DMG to modify the surface of oxidized copper in order to improve the subsequent adsorption of the more economically available BTA.

Indeed, it is able to stimulate BTA adsorption on copper by modifying its surface with a very small value Θ_{DMG}=0.1. On such a copper electrode, BTA adsorption begins in the range of its concentrations at which it does not yet occur on the passive copper surface without modification. This thin film provides better protection for copper in humid atmospheres than protection from BTA itself. Interestingly, in contrast to the above case for iron, a further increase in Θ_{DMG} does not enhance BTA adsorption and $\left(-\Delta G_a^0\right)$ remains at the level of 63 kJ/mol. The results of XPS studies led to the conclusion that DMG is bound to copper surface cations through two donor oxygen atoms of carboxyl groups. The DMG nitrogen atoms do not participate in the formation of coordination bonds with copper cations. The adsorbed DMG anions seem to have an oblique orientation with respect to the copper surface and can form several layers of CIs.

The study of DMG adsorption on nickel from the same borate buffer at E=–0.65 V (on the reduced surface) and 0.2 V (on the oxidized surface) also deserves attention [30]. In both cases, it was adequately described by the Temkin isotherm with values for E=−0.65 V: $\left(-\Delta G_a^0\right)$=75.38 kJ/mol and f=4, and for E=–0.2 V: $\left(-\Delta G_a^0\right)$=54.8 kJ/mol and f=2.8. It can be seen from the data that strong DMG chemisorption takes place on this metal as well, which is even more pronounced on the electrode with reduced nickel oxide.

As a surface modifier not only for copper, but also for its alloy MNZh5-1, there can be another porphyrin derivative – depocolin, that is, the disodium salt of 3,7,12,17-tetramethyl-8,13-divinyl-2,18-deuteroporphyrin IX (Figure 7b), depocolin (3,7,12,17-tetramethyl-8,13-divinyl-2,18-deuteroporphyrin IX) containing two peripheral carboxyl groups [31]. From the changes (–δΔ) during the adsorption of depocolin (Figure 9), the thicknesses of the formed monolayers on the surface of alloy MNZh5-1 and copper were calculated. It was found that on the oxidized surface of alloy MNZh5-1 and copper d~0.35 nm. Comparing the thickness of the emerging monolayer d and the length of the depocolin molecule l, calculated from the bond lengths of their constituents, it can be assumed that depocolin is adsorbed with a large inclination to the surface of both metals. The thickness of the depocolin layer on the alloy was also determined by the XPS method; it is about 0.3 nm (E=0.0 V) and 0.36 nm at a E_{corr}=0.12 V. The adsorption of depocolin from a neutral buffer solution on their oxidized surface is adequately described by the Temkin equation with the values $\left(-\Delta G_a^0\right)$=68 and 78 kJ/mol, respectively, in the case of copper and its alloy. The modification of the surface of copper and alloy MNZh5-1 with depocolin facilitates the subsequent adsorption of 5-Cl-BTA and passivation of these electrodes, increasing their protection in a neutral chloride solution from local depassivation. XPS data [32] showed that depocolin is bound to the surface of the alloy via the oxygen atoms of both carboxyl groups, and the porphyrin ring did not participate in the formation of the metal complex on the electrode.

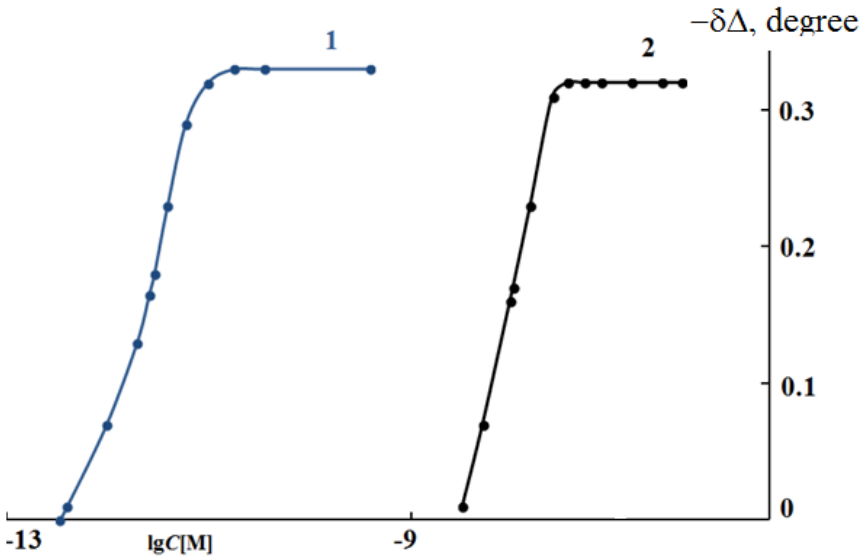

Figure 9. Dependence of the change in the ellipsometric angle (−δΔ) on the lg*C* of depocolin concentration on the oxidized surface of copper–nickel alloy MNZh 5-1 (1) and on copper surface (2) oxidized at $E=0$ V in borate buffer, pH 7.4.

Organophosphates

Organophosphates should be singled out among the anionic organic CIs, which are not only widely studied in neutral aqueous solutions, but have long been used in the practice of anticorrosion protection of metals. They include not only salts or complexes of phosphonic acids, but also other organic P-containing compounds. However, here we confine ourselves to phosphoric acid esters, which, of course, are used less frequently than phosphonates as CIs, but, undoubtedly, are also interesting in this function. Acid esters of phosphoric acid are distinguished not only by their ease of synthesis, but also by the relative stability of disubstituted esters, as well as their ability to form hydrophobic passive films on oxidized metal surfaces and complex compounds with cathions of many metals [33–35]. A good example of such CIs is dioctyl phosphate $(C_8H_{17}O)_2P(O)OHNa$ (DOPh) or its more branched isomer sodium bis(2-ethylhexyl)phosphate [36, 37]. DOPh proved to be one of the best water-soluble passivators for iron and mild steel in neutral solutions. The DOPh molecule is rather hydrophobic, as evidenced by its positive value log$P$=6.97, which exceeds that of, for example, the SPhU molecule (log$P$=5.89), which has high protective properties with respect to mild steel. For the anion DOPh log$D$=3.49. This value takes into account the acidity of the molecule, *i.e.* its dissociation and the pH of the solution. Indeed, the adsorption of DOPh from a borate buffer with pH 7.4 on pure iron [36] and on mild steel [37] at $E=0.2$ V is described by the Frumkin equation with the value $\left(-\Delta G_a^0\right)=28$ kI/mol.

The passivating properties of DOPh are manifested not only in relation to Fe and steels, but also to other metals or alloys. Thus, even in [35] the facilitation of passivation of zinc and aluminum alloy D16 in an aqueous solution of chlorides was observed upon the

introduction of DOPh. Other acidic organic esters of phosphoric acid also have adsorption activity on aluminum or its alloys.

In this regard, it is interesting to compare two surfactants – sodium dodecyl sulphate (SDS) and sodium dodecyl phosphate (SDP), carried out by F. Carlson *et al.* [38, 39]. The authors concluded that the effective corrosion inhibition caused by organophosphate anions may be due to their chemisorption, possibly including the formation of bridging bidentate complexes, as well as the ability to form stable complexes with Al(III). The adsorption behaviour was investigated by determination of the isotherms for adsorption of SDS and SDP at the aluminium pigment flakes. The inhibition tests with SDP clearly showed that phosphate ester surfactants provided efficient inhibition of the aluminium oxide surface.

S.V. Oleinik *et al.* [40] studied the adsorption of DOPh on the surface of D16 alloy in solutions of borate buffer (pH 7.4) by the ellipsometric method. Like in the study of CI adsorption on the magnesium surface [14], it was necessary to choose the conditions for surface preparation. The ellipsometric studies of the D16 alloy electrode in a borate buffer at E_{corr}=–0.3 V showed that Δ changes over a long time and does not reach a stationary value, probably due to the formation of a hydrated oxide of variable composition on the surface of the alloy. A technique was proposed in which thin passivating layers were preliminarily formed on the alloy. DOPh adsorption on such an electrode at E=–0.30 V is adequately described by the Frumkin equation with $\left(-\Delta G_a^0\right)$=33.8 kJ/mol. It follows from the analysis of the literature that the adsorption of mono- and dialkyl phosphates from aqueous solutions on magnesium or its alloys and their protective properties with respect to this metal have been studied to the least extent. Traditional methods of corrosion protection of magnesium alloys (chromate treatment and paintwork containing chromate pigments or CI) face serious environmental objections. Although chromate is the most studied and effective CI of magnesium alloys, toxicity and environmental hazard makes it necessary to replace its chromate in various technologies.

In this regard, it is interesting to compare the protective effect of potassium bichromate, DOPh and the well-known CI class of triazoles – 5-chloro-BTA (Cl-BTA) in relation to technical magnesium (Mg-90, containing (in%): Mg – 99.9; Fe≤0.04; Mn≤0.03; Al≤0.02; Ni≤0.001; Cu≤0.004; Si≤0.009; Cl≤0.005) in aqueous borate solutions with pH 7.4 and 9.2. As magnesium CI in aqueous solutions, 5-Cl-BTA and DOPh were studied [41]. The important role of DOPh in the protective effect of mixed CI is also indicated by the results of XPS studies carried out after keeping magnesium samples in water, since peaks of P2p electrons appeared in the spectrum. In all cases, they confirmed the presence of DOPh in the surface layers. In connection with the assumption of DOPh chemisorption on the oxidized magnesium surface, it seemed interesting to estimate the free energy of adsorption of this CI on it by measuring the DOPh isotherm by the in situ method. In the range of average coverages, it is adequately described by the logarithmic Temkin isotherm with close values for these compounds $\left(-\Delta G_a^0\right)$=50.2 kJ/mol. However, the 5-Cl-BTA anions are located

obliquely to the electrode surface, while the DOPh anions are located vertically, which suggests its denser packing. DOPh additions lead not only to a shift in the local depassivation potential, but also to a decrease in the anode current.

Phosphonic acids are capable of complex formation with ions of various metals, including Zn^{2+}, forming thin passivating films on the metal surface. Phosphonic acids are capable of imparting various physical and chemical properties to ZnO nanoparticles, depending on the nature of their tail group. So, it can increase the hydrophobicity of the surface when it ends with an alkyl, and vice versa, reduce it when the tail group is an acid. In addition, hydrogen bonding between acid end groups enhances film stabilization [42, 43].

Adsorption of sodium salt of decylphosphonic acid $CH_3(CH_2)_9PO(ONa)_2$ (SDPh) and of dodecylphosphonic acid $CH_3(CH_2)_{11}PO(ONa)_2$ (SDDPh) on a zinc surface from a borate buffer solution pH 7.4 was investigated in [44, 45]. The adsorption of SDPh on the oxidized and reduced zinc surface can be described by the Temkin equation. On the reduced surface, SDPh is adsorbed more easily than on the oxidized one: at E=–0.9 V, the value of $\left(-\Delta G_a^0\right)$=75.8 kJ/mol, and at E=0.2 V $\left(-\Delta G_a^0\right)$=42.2 kJ/mol. SDDPh is adsorbed only at E=–0.9 V with $\left(-\Delta G_a^0\right)$=85.7 kJ/mol. The thickness of the adsorbed SDDPh monolayer is d=1.7 nm. The length of the SDDPh molecule is 1.79 nm. Comparing these dimensions, we can assume that the SDDPh molecules are oriented almost perpendicular to the electrode surface.

In [46], the kinetics of adsorption and desorption of organophosphoric CIs on the surface of steel OL-37 was studied. These are the organophosphonate CIs: amino trimethylenephosphonic acid and 1-hydroxyethylidene-1,1-diphosphonic acid. The concentrations of the CI solutions were 1%. The steel plate was placed for 40 min in the CI solution. The ellipsometric parameters of the plate were measured before and after immersion. From this data, the thickness of the CI film was calculated. During desorption of CI, the value of Δ increases, while the value of Ψ decreases as the thickness of its film decreases. The measured refractive index of the CI film is N_{film}=1.63. Desorption of CI from the plates was determined in the air.

Azoles

Azoles are five-membered heterocyclic compounds that have at least two heteroatoms in the cycle, one of which is a nitrogen atom, as well as bi- and polycyclic compounds that include an azole ring. Review [47] is devoted to azoles, a popular class of heterocyclic CIs that have been best studied. The adsorption of substituted benzotriazoles (R-BTAs) onto copper is measured via ellipsometry in a pure borate buffer (pH 7.4) [48]. Commercially available CIs for copper, BTA and its derivatives, 5-chloro-, 5-methyl-, and 5-pentyl-benzotriazoles with the general structural formula $R\text{-}C_6H_4N_3$, were employed. Figure 10 shows the experimental dependence of the absolute values of $\delta\Delta$ on log$C$, where C_{inh} is the volume concentration of the studied CIs in the borate buffer. The values of log$P$, B_{max}, B_{min}, $\left(-\Delta G_{a,max}^0\right)$, $\left(-\Delta G_{a,min}^0\right)$

are given in Table 3. B_{max} and B_{min} are the constants of adsorption equilibrium that correspond to the highest and lowest values of the free energy of adsorption.

Table 3. Acid dissociation constant of pK_a; partition coefficients (log$P$); and parameters (B_{max}), and (B_{min}) as functions of the chemical structure of CIs belonging to the benzotriazoles family. The pK_a and log$P$ values were determined using the ACDLABS software.

Inhibitors	**pK_a**	**log$P$**	**B_{max} mol^{-1}**	**B_{min} mol^{-1}**	**$\left(-\Delta G^0_{a,min}\right)$ kJ/mol**	**$\left(-\Delta G^0_{a,max}\right)$ kJ/mol**
BTA	8.38	1.29	$23.2\cdot10^8$	$17.2\cdot10^8$	51.8	52.5
5-CH_3-BTA	8.70	1.61	$3.7\cdot10^{10}$	$2.7\cdot10^{10}$	58.5	59.2
5-Cl-BTA	5.46	1.92	$9.5\cdot10^{10}$	$3.8\cdot10^{10}$	59.3	61.5
5-C_5H_{11}-BTA	9.4	3.19	$20.5\cdot10^{11}$	$7.2\cdot10^{11}$	66.4	69.1

After the formation of a conditional monolayer, further changes in the ellipsometric angle Δ occur in time. This is due to the fact that copper cations, slowly accumulating in solution, form complex compounds with CI, which begin to be adsorbed and form the second and subsequent layers. For this reason, the formation of the second layer is shown on the isotherms by a dotted line (Figure 10). Free energy of adsorption $\left(-\Delta G^0_{a,max}\right)$ increases in the order BTA<5-CH_3-BTA<5-Cl-BTA<5-C_5H_{11}-BTA, which coincides with the order of the increase in the hydrophobicity of these compounds.

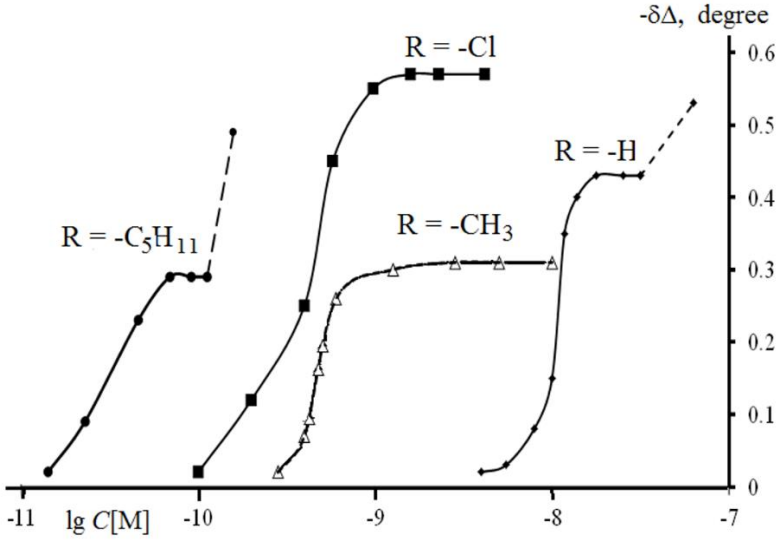

Figure 10. Changes in ellipsometric angle Δ as a function of the concentration of BTA and its derivatives on copper surface oxidized at E=0 V in borate buffer, pH 7.4. The regions of nonstationary angle Δ values are shown in the curves as dashed lines.

The adsorption of BTA, tolyltriazole (TTA) and two different *N*-methylamino substituted triazoles on copper surfaces in hydrocarbon media has been examined by *in situ* ellipsometry and time-of-flight secondary ion mass spectroscopy [49]. It was shown that all four triazoles form films, and according to ellipsometric measurements, their thickness, *d*, after a 1000-minute exposure of the samples was estimated in the range of 0.5–2 nm. The films formed by BTA and TTA had $d \sim 2$ nm, and in the case of *N*-methylamino substituted triazoles, $d \sim 0.5$ nm. Desorption was studied only qualitatively, but it was shown that no more than 20% of CI was desorbed. The time-of-flight secondary ion mass spectroscopy study showed that while BTA and TTA adsorbed intact did the N-aminomethyl substituted triazoles appear to loose their aminomethyl tails on binding since only signals corresponding to triazole moieties of the compounds were detected.

Not only BTA derivatives but also 3-amino-triazole (3-AT) derivatives can be excellent CIs for copper in neutral media. In our work [50], using ellipsometry and electrochemical measurements, we studied the adsorption of 3-amino-1,2,4-triazoles (3-AT) and its substituted derivatives on copper, as well as their effect on its dissolution in aqueous solutions of a borate buffer with pH 7.4. It is shown that the adsorption of these triazoles on copper at $E = 0.0$ V is polymolecular, and the first layer is described by the Temkin equation $\left(-\Delta G_a^0\right) = 57-77$ kJ/mol and an energy inhomogeneity coefficient varying from 0.91–2.5 (Table 4). The maximum value of $\left(-\Delta G_a^0\right)$ is found for an acid and a hydrogen sulfide corrosion inhibitor IFKhAN-92 that is a mixture of triazole derivatives.

Table 4. Dependence of *f* and $\left(-\Delta G_a^0\right)$ parameters on the chemical structure of the inhibitors.

Corrosion inhibitor	B_{max}, mol^{-1}	B_{min}, mol^{-1}	$\left(-\Delta G^0_{a,min}\right)$, kJ/mol	$\left(-\Delta G^0_{a,max}\right)$, kJ/mol	***f***
IFKhAN-92	66.6×10^{12}	26.6×10^{12}	75.2	77.4	0.91
5-Pentylmercapto-3-AT	18.31×10^{12}	4.4×10^{12}	70.9	74.3	1.42
5-Phenyl-3-AT	15.04×10^{10}	1.3×10^{10}	56.6	62.6	2.47
3-AT	2.00×10^{10}	7.0×10^{9}	55.2	57.7	1.04

All the compounds studied are strongly chemisorbed on copper and, judging by the measured adsorption parameters, the well-known inhibitor of acid and hydrogen sulfide corrosion of steel IFKhAN-92 is most studied in [51]. It is also least sensitive to the energy inhomogeneity of the copper surface. This CI is a composition of 3-AT derivatives and has a high passivating ability with respect to copper while protecting it from atmospheric corrosion. The existence of the IFKhAN-92 chemisorbed layer on copper was confirmed by the fact that the kinetic adsorption isotherm of this CI observed by the authors is adequately described by the Roginsky–Zeldovich equation obtained theoretically for slow chemisorption [52].

In our other work [53], we studied the adsorption of 5-alkyl derivatives of 3-AT and the protection of copper from atmospheric corrosion. In these, the alkyls were methyl-, pentyl-, heptyl-, nonyl- and undecyl-, which allowed these CIs to form passive layers on the copper surface at very low concentrations in the range of a few μM. At higher concentrations, this effectively inhibited local depassivation of copper by chlorides in neutral borate buffer pH 7.4. An increase in the length of the side chain enhances the action of 5-alkyl-3-AT, but reduces their solubility in water.

The adsorption of 5-alkyl-3-AT is adequately described by the Temkin equation, and the values of $\left(-\Delta G_{\mathrm{a}}^{0}\right)$ increase with increasing alkyl length. Protective films formed by higher 5-alkyl-3-ATs provide reliable protection of copper against corrosion even under severe salt fog conditions. Moreover, mixtures of some 3-alkyl-ATs are able to show higher efficiency than each of the components separately. In [54], ellipsometry has been used to determine the thickness and growth rate of protective copper–benzotriazole (Cu–BTA) and copper–benzimidazole (Cu–BIMDA) surface films formed on CuO/Cu substrates by immersion in warm (60°C) aqueous (0.017 mol/L) solutions of BTA and BIMDA. The growth rate of Cu–BTA films is found to be significantly smaller than that of (Cu–BIMDA) films. In case of immersion for 3 min, the Cu–BTA and Cu–BI films grow to thicknesses of about 100 Å in about 475 Å, respectively. A possible explanation of the generally greater protective properties of Cu–BTA compared with Cu–BIMDA is discussed.

Similar studies are also presented in [55] where the well-known CI for the protection of copper and its alloys, 2-mercaptobezothiazole (MBT), was studied. In this study, a thin anticorrosion coating obtained from MBT solutions on a copper surface is analyzed by spectral ellipsometry. It is shown that it is rapidly formed on the Cu_2O layer at temperatures above 50°C.

The interaction of 2-mercaptobenzothiazole with copper was also studied in an alkaline solution in [56] using infrared (IR) and Raman spectroscopy and in situ ellipsometry combined with cyclic voltammetry (CV). At a constant electrode potential, the MBT film relaxes with a change in the orientation of its molecules. In this film, the thiol form of MBT predominates over the thionic form. After the dissolution of copper becomes thermodynamically possible, including in the case of an open circuit, the formation of a multilayer CuMBT complex begins, in which thiol predominates over thione. In this case, MBT molecules bind to copper through S and N atoms. At positive potentials, the formation of a disulfide oxidation product of MBT itself prevents this reaction of the copper surface. Multilayer films effectively retard oxide formation. Instead, MBT oxidizes and dimerizes to 2,2′-dibenzothiazole disulfide (DBTS), which retains copper protection. The authors concluded that MBT acts as a “sacrificial inhibitor” because its molecule is oxidized instead of copper.

The behavior of zinc in alcoholic solutions of BTA was studied in [57]. The authors note a good agreement between the thickness of the upper layer between the results of ellipsometry and the intensities of the XPS peaks calculated using the Seah model.

The adsorption, protective, and passivation effects of 1,2,4-triazole, 3-amino-1,2,4-triazole, and 5-COOH-3-AT in a neutral borate buffer solution with pH 7.4 were studied on zinc [58]. Adsorption isotherms were calculated from the full Temkin isotherm. It is shown that 5-COOH-3-AT anions have higher values of adsorption free energy $\left(-\Delta G_a^0\right)$ on zinc at E=0.2 V compared to triazole and 3-amino-1,2,4-triazole respectively. 82.2, 49.6 and 43.8 kJ/mol. Corrosion testing of zinc in an aqueous chloride solution for 7 days showed that 5-COOH-3-AT at 7 mmol/L reduces the corrosion rate by a factor of 7.5 and provides a degree of protection close to 90%.

Conclusions

After analyzing the results obtained by us and cited in the literature on the study of adsorption by the ellipsometric method of CIs in aqueous media, it can be stated that this method is unique in its ability to obtain adsorption isotherms and determine adsorption constants. The combination with electrochemical measurements makes it possible to study adsorption in a wide range of potentials. We have studied the adsorption of CIs on the surface of zone-melted Fe, Fe-Armco, St3, Cu, MNZh5-1 alloy, Ni, Ag, Al, Au, and Mg from aqueous media. CIs such as sodium salts of carboxylic and dicarboxylic acids, phosphonic acids, acid dialkyl phosphates, and azoles have been studied. Examples of adsorption of a mixture of CIs, induced adsorption are given. The possibility of enhancing the adsorption of BTA by small fractions of dimegin on iron and copper is shown. Depokolin was proposed as a surface modifier for copper and MNZh5-1 alloy. In many cases, studies of carboxylate CIs identified relationships between their hydrophobicity and the value of the free energy of adsorption. The conditions for preparing the surface of magnesium and aluminum in order to obtain adsorption isotherms on their surfaces are considered in detail. Adsorption isotherms of sodium salts of higher carboxylic acids were obtained on magnesium: sodium oleyl sarcosinate, sodium oleate, linoleate from a borate solution pH 11.2. Determination of the thicknesses of the adsorbed layers suggests their location on the surface. The thicknesses determined by the ellipsometric method and XPS coincide within the measurement error. For some CIs, kinetic adsorption isotherms have been obtained, which can be adequately described by the Roginsky–Zeldovich equation obtained for the case of slow chemisorption. This may be another argument in favor of their chemisorption.

References

1. N.P. Andreeva, Yu.I. Kuznetsov and Kh.S. Shikhaliev, The use of ellipsometry for studying adsorption of organic corrosion inhibitors from aqueous solutions on metals. Review. Part 1. Methods for obtaining adsorption isotherms, *Int. J. Corros. Scale Inhib.*, 2022, **11**, no. 4, 1716–1723. doi: 10.17675/2305-6894-2022-11-4-20
2. Yu.I. Kuznetsov, A.D. Mercer and J.G.N. Thomas, *Organic Inhibitors of Corrosion of Metals*, Plenum Press: New York and London, 1996, 283. doi: 10.1007/978-1-4899-1956-4

3. Yu.I. Kuznetsov, Organic corrosion inhibitors: where are we now? A review. Part I. Adsorption, *Int. J. Corros. Scale Inhib*., 2015, **4**, no. 4, 284–310. doi: 10.17675/2305-6894-2015-4-4-1
4. Yu.I. Kuznetsov, Organic corrosion inhibitors: where are we now? A review. Part II. Passivation and the role of chemical structure of carboxylates, *Int. J. Corros. Scale Inhib*., 2016, **5**, no. 4, 282–318. doi: 10.17675/2305-6894-2016-5-4-1
5. Ya.G. Bober, Yu.I. Kuznetsov and N.P. Andreeva, Adsorption at Iron and Passivation Effect of Anions of Substituted Phenylanthranilic Acids, *Prot. Met*., 2008, **44**, no. 1, 84–90. doi: 10.1134/S0033173208010116
6. C. Hansch and A. Leo, *Substituent Constants for Correlation Analysis in Chemistry and Biology*, Wiley-Interscience: New York, 1979, 339.
7. L.P. Hammet, *Physical Organic Chemistry*, 1970, New York: McGraw -Hill Book Company G.T.
8. R.A. Scherrer and S.M. Howard, Use of distribution coefficients in quantitative structure-activity relations, *J. Med. Chem*., 1977, **20,** no. 1, 53–58. doi: 10.1021/jm00211a010
9. L.P. Kazansky, Yu.I. Kuznetsov, N.P. Andreeva and Y.G. Bober, Self-assembled monolayers of flufenaminate anions on mild steel surface formed in aqueous solution, *Appl. Surf. Sci*., 2010, **257**, no. 4, 1166–1174. doi: 10.1016/j.apsusc.2010.07.077
10. Yu.I. Kuznetsov, N.P. Andreeva, N.P. Sokolova and R.A. Bulgakova, Joint adsorption of oleic and phenylanthranilic acids at passive iron, *Prot. Met*., 2003, **39**, no. 5, 462–467. doi: 10.1023/A:1025898803486
11. Yu.I. Kuznetsov and N.P. Andreeva, Adsorption of Organic Anions on Iron in Aqueous Solutions: An Ellipsometric Study, *Russ. J. Electrochem*., 2006, **42**, no. 10, 1101–1106. doi: 10.1134/S102319350610017X
12. Yu.I. Kuznetsov, N.P. Andreeva and M.O. Agafonkina, On co-adsorption on passive iron from aqueous 1,2,3-benzotriazole and sodium phenylundecanoate, *Russ. J. Electrochem*., 2010, **46**, no. 5, 560–564. doi: 10.1134/S1023193510050101
12. B.B. Damaskin, A.N. Frumkin and N.A. Borovaya, The influence of a constant concentration of a surface-active component on the shape of the adsorption isotherm of another substance, *Electrochemistry*, 1972, **8**, no. 6, 807–815 (in Russian).
14. V.A. Ogorodnikova, Yu.I. Kuznetsov, N.P. Andreeva, A.Y. Luchkin and A.A. Chirkunov, Adsorption of anions of higher carboxylic acids on magnesium from weakly alkaline aqueous solutions, *Russ. J. Phys. Chem. A*, 2020, **94**, no. 6, 1104–1110. doi: 10.1134/S0036024420060187
15. M.O. Agafonkina, A.M. Semiletov, Yu.I. Kuznetsov, N.P. Andreeva and A.A. Chirkunov, Adsorption of Sodium Oleyl Sarcosinate on Zinc and Its Passivating Action in Neutral Aqueous Solution, *Prot. Met. Phys. Chem. Surf*., 2018, **54**, no. 7, 1284–1291. doi: 10.1134/S207020511807002X

16. N.P. Andreeva, Yu.V. Ushakova, Yu.I. Kuznetsov, M.O. Agafonkina, L.P. Kazansky and Yu.Ya. Andreev, Adsorption of sodium flufenaminate on zinc from aqueous solutions, *Prot. Met. Phys. Chem. Surf*., 2014, **50**, no. 7, 860–865. doi: 10.1134/S2070205114070041
17. Yu.I. Kuznetsov, M.O. Agafonkina and N.P. Andreeva, Inhibitor Properties of Carboxylates and Their Adsorption on Copper from Aqueous Solutions, *Russ. J. Phys. Chem. A*, 2015, **89**, no. 6, 1070–1076. doi: 10.1134/S0036024415060023
18. I.L. Knunyants, *Chemical Encyclopedia*, Moscow, The Great Russian Encyclopedia, 1995, 580 (in Russian).
19. E. Rocca, G. Bertrand, C. Rapin and J.C. Labrune, Inhibition of copper aqueous corrosion by non-toxic linear sodium heptanoate: mechanism and ECAFM study, *J. Electroanal. Chem*., **503**, no. 1–2, 133–140. doi: 10.1016/S0022-0728(01)00384-9
20. N. Stein, L. Johann, C. Rapin and J.M. Lecuire, *In-situ* ellipsometric study of copper passivation by copper heptanoate through electrochemical oxidation, *Electrochim. Acta*, 1998, **43,** no. 21–22, 3227–3232. doi: 10.1016/S0013-4686(98)00053-X
21. G.T. Hefter, N.A. North and S.H. Tan, Organic corrosion inhibitors in neutral solutions. Part 1. Inhibition of steel, copper and aluminum by straight chain carboxylates, *Corrosion*, 1997, **53**, no. 8, 657–667. doi: 10.5006/1.3290298
22. M.O. Agafonkina, I.A. Kuznetsov, N.P. Andreeva and Yu.I. Kuznetsov, Copper protection with sodium salts of lower dicarboxylic acids in neutral aqueous solution, *Int. J. Corros. Scale Inhib*., 2020, **9**, no. 3, 1000–1013. doi: 10.17675/2305-6894-2020-9-3-13
23. I.A. Kuznetsov, A.A. Chirkunov, Yu.I. Kuznetsov, Kh.S. Shikhaliev, M.O. Agafonkina, N.P. Andreeva and Yu.A. Kovygin, Protection of copper against corrosion in neutral solutions by salts of 2-alkylmalonic acids, *Int. J. Corros. Scale Inhib*., 2022, **11**, no. 3, 1401–1417. doi: 10.17675/2305-6894-2022-11-3-29
24. M.A. Quraish and J. Rawat, A review on macrocyclics as corrosion inhibitors, *Corros. Rev*., 2001, **19,** no. 3–4, 273–300. doi: 10.1515/CORRREV.2001.19.3-4.273
25. O.Yu. Grafov and L.P. Kazansky, Review on porphyrins, phthalocyanines and their derivatives as corrosion inhibitors, *Int. J. Corros. Scale Inhib*., 2020, **9**, no. 3, 812–829. doi: 10.17675/2305-6894-2020-9-3-2
26. K.S. Lokesh, M.De Keersmaecker, A. Elia, D. Depla, P. Dubruel, P. Vandenabeele, S. Van Vlierberghe and A. Adriaens, Adsorption of cobalt (II) 5,10,15,20-tetrakis(2-aminophenyl)-porphyrin onto copper substrates: Characterization and impedance studies for corrosion inhibition, *Corros. Sci*., 2012, **62**, 73–82. doi: 10.1016/j.corsci.2012.04.037
27. O.K. Özdemir, A. Aytaç, D. Atilla and M. Durmuş, Corrosion inhibition of aluminum by novel phthalocyanines in hydrochloric acid solution, *J. Mater. Sci*., 2011, **46**, 752–758. doi: 10.1007/S10853-010-4808-6

28. Yu.I. Kuznetsov, N.P. Andreeva, M.O. Agafonkina and A.B. Colov'eva, Modification of Iron Surface by Dimegin and Adsorption of 1,2,3-Benzotriazole, *Prot. Met. Phys. Chem. Surf*., 2010, **46**, no. 7, 743–747. doi: 10.1134/S2070205110070014
29. Yu.I. Kuznetsov, M.O. Agafonkina, N.P. Andreeva and L.P. Kazansky, Adsorption of dimegin and inhibition of copper dissolution in aqueous solutions, *Corros. Sci*., 2015, **100**, 535–543. doi: 10.1016/j.corsci.2015.08.028
30. O.Yu. Grafov, M.O. Agafonkina, N.P. Andreeva, L.P. Kazanskii and Yu.I. Kuznetsov, Adsorption of Depocolin and Dimegin on Nickel from Neutral Aqueous Solutions, *Prot. Met. Phys. Chem. Surf*., 2019, **55,** no. 7, 1304–1310. doi: 10.1134/S2070205119070074
31. M.O. Agafonkina, O.Yu. Grafov, N.P. Andreeva, L.P. Kazanskii and Yu.I. Kuznetsov, Modifying Copper and Copper Alloy Surface with Depocolin and 5-Chloro-1,2,3-Benzotriazole from a Neutral Aqueous Solution, *Russ. J. Phys. Chem. A*, 2021, **95**, 2295–2303. doi: 10.1134/S0036024421110029
32. O.Yu. Grafov, L.P. Kazansky, S.V. Dubinskaya and Yu.I. Kuznetsov, Adsorption of depocolin and inhibition of copper dissolution in aqqueous solutions, *Int. J. Corros. Scale Inhib*., 2019, **8**, no. 3. 549–559. doi: 10.17675/2305-6894-2019-8-3-6
33. A.V. Fokin, M.V. Pospelov and A.N. Levichev, Oil-soluble corrosion inhibitors. Mechanism of action and compositions used, *Results of science and technology, Series: Corrosion and corrosion protection*, 1984, **10**, 3–77 (in Russian).
34. P.G. Mingalyov and G.V. Lisichkin, Chemical modification of oxide surfaces with organophosphorus(v) acids and their esters, *Russ. Chem. Rev*., 2006, **75**, no. 6, 541–557. doi: 10.1070/RC2006v075n06ABEH002478
35. Yu.I. Kuznetsov, Organic corrosion inhibitors: where are we now? A review. Part III. Passivation and the role of the chemical structure of organophosphates, *Int. J. Corros. Scale Inhib*., 2017, **6**, no. 3, 209–239. doi: 10.17675/2305-6894-2017-6-3-1
36. Yu.I. Kuznetsov, N.P. Andreeva and G.Yu. Kazanskaya, On the Inhibition Effect of Dialkyl Phosphates in the Depassivation of Metals, *Prot. Met*., 2000, **36**, no. 4, 351–355. doi: 10.1007/BF02758507
37. A.A. Chirkunov, A.S. Gorbachev, Yu.I. Kuznetsov and N.P. Andreeva, Adsorption of Dioctyl Phosphate and Inhibition of Dissolution of Low-Carbon Steel in Neutral Solution, *Prot. Met. Phys. Chem. Surf*., 2013, **49**, no. 7, 854–858. doi: 10.1134/S2070205113070058
38. P.M. Karlsson, A. Baeza, M.W. Anderson and A.E.C. Palmqvist, Surfactant inhibition of aluminium pigments for waterborne printing inks, *Corros. Sci*., 2008, **50**, no. 8, 2282–2287. doi: 10.1016/j.corsci.2008.06.014
39. P.M. Karlsson, B.R. Postmus and A.E.C. Palmqvist, Dissolution and Protection of Aluminium Oxide in Corrosive Aqueous Media – An Ellipsometry and Reflectometry Study, *J. Dispersion Sci. Technol*., 2009, **30**, 949–953. doi: 10.1080/01932690802646363

40. S.V. Oleinik, Yu.A. Kuzenkov, N.P. Andreeva and Yu.I. Kuznetsov, Spineless pigments to protect the aluminum alloy D16, *Korroz.: Mater., Zashch. (Corrosion: materials, protection)*, 2008, no. 3, 29–34. (in Russian).
41. N.P. Andreeva, Yu.I. Kuznetsov, A.M. Semiletov and A.A. Chirkunov, The formation of passive films on magnesium in alkaline solutions and adsorption of anions of organic acids on them, *Prot. Met. Phys. Chem. Surf.*, 2018, **54**, no. 7, 1338–1345. doi: 10.1134/S2070205118070043
42. S. Manov, A.M. Lamazouere and L. Aries, Electrochemical study of the corrosion behaviour of zinc treated with a new organic chelating inhibitor, *Corros. Sci*., 2000, **42**, no. 7, 1235–1348. doi: 10.1016/S0010-938X(99)00132-8
43. M. Troquet, J.P. Labbe and J. Pagetti, The mechanism of the inhibition of zinc corrosion in 1N HCl solution by tetraphenylphosphonium bromide, *Corros. Sci*., 1981, **21**, no. 2, 101–117. doi: 10.1016/0010-938X(81)90095-0
44. Yu.I. Kuznetsov, G.V. Red'kina and N.P. Andreeva, Adsorption from neutral solutions of sodium alkyl phosphonates on zinc and its passivation, *Russ. J. Phys. Chem. A*, 2018, **92**, no. 12, 2548–2555. doi: 10.1134/S0036024418120269
45. G.V. Redkina, Yu.I. Kuznetsov, N.P. Andreeva, I.A. Arkhipushkin and L.P. Kazansky, Features of zinc passivation by sodium dodecylphosphontate in a neutral aqueous solution, *Corros. Sci*., 2020, **168**, 108554. doi: 10.1016/j.corsci.2020.108554
46. S. Jitian, The ellipsometrical study of adsorption-desorption of the corrosion inhibitors on metallic surfaces, *Rom. Rep. Phys*., 2013, **65**, no. 1, 204–212.
47. Yu.I. Kuznetsov and L.P. Kazansky, Physicochemical aspects of metal protection by azoles as corrosion inhibitors, *Russ. Chem. Rev*., 2008, **77**, no. 3, 219–232. doi: 10.1070/RC2008v077n03ABEH003753
48. M.O. Agafonkina, N.P. Andreeva, Yu.I. Kuznetsov and S.F. Timashev, Substituted Benzotriazoles as Inhibitors of Copper Corrosion in Buffer Borate Solutions, *Russ. J. Phys. Chem. A*, 2017, **91**, no. 8, 1410–1417. doi: 10.1134/S0036024417080027
49. M. Levin, P. Wiklund and H. Arwin, Adsorption and film growth of *N*-methylamino substi-tuted triazoles on copper surfaces in hydrocarbon media, *Appl. Surf. Sci*., 2007, **254**, no. 5, 1528–1533. doi: 10.1016/j.apsusc.2007.07.023
50. Yu.I. Kuznetsov, Kh.S. Shikhaliev, M.O. Agafonkina, N.P. Andreeva, A.M. Semiletov, A.A. Chirkunov, A.Yu. Potapov and V.E. Solov'ev, Formation of Passivating Layers by 1,2,4-Triazole Derivatives on Copper in Aqueous Solutions, *Russ. J. Phys. Chem. A*, 2017, **91**, no. 12, 2458–2465. doi: 10.1134/S0036024417120147
51. Ya.G. Avdeev, M.V. Tyurina and Yu.I. Kuznetsov, Protection of low-carbon steel in phosphoric acid solutions by mixtures of a substituted triazole with sulfur-containing compounds, *Int. J. Corros. Scale Inhib*., 2014, **3**, no. 4, 246–253. doi: 10.17675/2305-6894-2014-3-4-246-253
52. S.Z. Roginsky and Ja. Zeldovich, The catalytic oxidation of carbon monoxide on manganese dioxid, *Acta Physicochim. URSS*, 1934, **1**, no. 3–4, 554–594.

53. A.A. Chirkunov, Yu.I. Kuznetsov, Kh.S. Shikhaliev, M.O. Agafonkina, N.P. Andreeva, L.P. Kazansky and A.Yu. Potapov, Adsorption of 5-alkyl-3-amino-1,2,4-triazoles from aqueous solutions and protection of copper from atmospheric corrosion, *Corros. Sci*., 2018, **144**, 230–236. doi: 10.1016/j.corsci.2018.08.056
54. N.D. Hobbins and R.F. Roberts, An ellipsometric study of thin films formed on copper by aqueous benzotriazole and benzimidazole, *Surf. Technol*., 1979, **9**, no. 4, 235–239. doi: 10.1016/0376-4583(79)90098-0
55. H. Nishizawa, O. Sugiura, Yo. Matsumura and M. Kinoshita, Evaluation of Mercaptobenzothiazole Anticorrosive Layer on Cu Surface by Spectroscopic Ellipsometry, *Jpn. J. Appl. Phys*., 2007, **46**, no. 5, 2892. doi: 10.1143/JJAP.46.2892
56. Y.H. Chen and A. Erbe, The multiple roles of an organic corrosion inhibitor on copper investigated by a combination of electrochemistry-coupled optical in situ spectroscopies, *Corros. Sci*., 2018, **145**, 232–238. doi: 10.1016/j.corsci.2018.09.018
57. V. Sirtori, F. Zambon and L. Lombardi, XPS and ellipsometric characterization of zinc-BTA complex, *J. Electron. Mater*., 2000, **29**, no. 4, 463–467. doi: 10.1007/s11664-000-0162-9
58. M.O. Agafonkina, Yu.I. Kuznetsov and N.P. Andreeva, Adsorption and protective properties of 1,2,4-triazole derivatives on zinc in a neutral chloride solution, *Korroz.: Mater., Zashch. (Corrosion: materials, protection)*, 2021, no. 7, 11–19. doi: 10.31044/1813 (in Russian).

♦ ♦ ♦